Cover Sheet

This file is the final accepted manuscript for the following paper:

ANISOtime: Traveltime Computation Software for Laterally Homogeneous, Transversely Isotropic, Spherical Media
By Kensuke Konishi, Anselme F. E. Borgeaud, Kenji Kawai, Robert J. Geller
Publisher: Seismological Society of America
Published: 14 July 2021
Seismological Research Letters (2021) 92 (6): 3811–3820.
DOI: https://doi.org/10.1785/0220200306

Access to ANISOtime software

ANISOtime can be downloaded from https://github.com/UT-GlobalSeismology/anisotime.

Downloadable executable versions are available for Windows, macOS, and Unix/Linux; the source code can also be downloaded. A user guide can be downloaded from this site, and is also embedded in the software.

ANISOtime: Traveltime computation software for laterally homogeneous, transversely isotropic, spherical media

Kensuke Konishi[1], Anselme F. E. Borgeaud[1,2], Kenji Kawai[2], and Robert J. Geller*[2]

[1]Institute of Earth Sciences, Academia Sinica, 11529 Taipei, Taiwan.

[2]Department of Earth and Planetary Science, School of Science, University of Tokyo, Hongo 7-3-1, Bunkyo-ku, Tokyo 113-0033 Japan.

May 7, 2021

Declaration of Competing Interests: The authors acknowledge there are no conflicts of interest recorded.

ABSTRACT

Software packages for computing seismic traveltimes and raypaths in an isotropic, spherically symmetric, Earth model are well known and widely used. However,

*Corresponding Author. email: bob@eps.s.u-tokyo.ac.jp

even though the theory for transversely isotropic (TI), spherically symmetric, models has been known since the late 1960s, readily available programs for traveltime calculations are restricted to isotropic models. We have developed a new software package, *ANISOtime*, for computing seismic traveltimes and raypaths in laterally homogeneous, transversely isotropic (TI), spherical media. This package calculates traveltime tables for both immediate and subsequent use. *ANISOtime* has both graphical user interface (GUI) and command-line interface (CLI) modes. The package is available for free public download. As it offers cross-platform compatibility through Java 8, it runs on Windows, macOS, and Unix/Linux.

INTRODUCTION

Traveltime computation is required widely in seismology. Although the Earth is laterally heterogeneous, the starting point for much research and teaching is traveltime computation for a laterally homogeneous, isotropic, model. The *TauP Toolkit* (Crotwell *et al.*, 1999) is well known as a reliable and readily usable public software package for traveltime and raypath computations for arbitrary spherically symmetric, isotropic velocity models.

The importance of anisotropy in seismological research is steadily increasing. For example, inferring anisotropy in the mantle allows inferences to be drawn about the direction of mantle flow. Inferring anisotropy is also an important research topic in exploration seismology. Use of *ANISOtime* can contribute to such research. It can also be used in introductory seismology courses to give students some exposure to basic concepts of anisotropy. A sample homework exercise is available from the GitHub page for *ANISOtime*.

As is well known (Love, 1927; Crampin, 1981), the most general anisotropic elastic medium has 21 independent elastic constants, while an isotropic elastic medium has just two, λ (or κ) and μ. In this paper we consider transversely isotropic (TI) media with a vertical symmetry axis (sometimes called VTI media). The basic theory for such media is well known (Vlaar, 1968, 1969; Woodhouse, 1981), but to our knowledge, no readily available public software package can handle traveltime calculations for transversely isotropic media.

We have developed a free public software package, *ANISOtime*, for making traveltime calculations for a spherically symmetric, TI, medium. *ANISOtime* takes advantage of the cross-platform benefits of the Java language and has both graphical user interface (GUI) and command line interface (CLI) modes.

THEORY

As noted above, the basic theory for computing traveltimes in a transversely isotropic medium with a vertical symmetry axis is well known, and *ANISOtime* uses these results. The three basic types of body-waves in such a medium are called pseudo-P, pseudo-SV, and SH, respectively. The "pseudo" for the first and second wave types is because they are not strictly longitudinal and transverse.

To make this paper self-contained, we present a derivation of the theory in Text S1 of the supplemental material. This may be a useful supplementary text for use in introductory courses. All variables used in the main body of this paper are listed in Table 1 in order of their appearance. For purposes of the theoretical derivations the ray parameter p has units of s/radian, the epicentral distance Δ is in radians, and all other variables are in SI units, but for convenience the density ρ is in g/cm^3, the radius r is in km, the velocities are in km/s, the epicentral distance Δ is in degrees, and the ray parameter p is in s/degree in the input to *ANISOtime*.

ANISOtime computes traveltime T and epicentral distance Δ for a spherical model as follows:

$$\Delta(p) = \int q_\Delta(p,r)\ dr \tag{1}$$

$$T(p) = \int q_T(p,r)\ dr, \tag{2}$$

where the kernels are defined in eqs. (S72)–(S77) in the supplemental material. The above integrations are computed by Simpson's rule (with the exception of the layer at the turning point, see below) for a given integral mesh ($r_1, r_2, ...,$ where $r_i < r_{i+1}$) as follows:

$$\Delta(p) = \sum_i \int_{r_i}^{r_{i+1}} q_\Delta(p,r)\ dr \tag{3}$$

$$T(p) = \sum_i \int_{r_i}^{r_{i+1}} q_T(p,r)\ dr. \tag{4}$$

The computational mesh can be arbitrary. Our default mesh spacing is 1 km.

In order to perform the integration accurately, special care must be taken in handling the integration near the turning point of a raypath, where the kernel $q_\tau \to 0$, and the integrands become singular but integrable. In *ANISOtime*, the integration for the interval bounded by the turning point is computed following Jeffreys and Jeffreys (1956, p. 288–290), as is also done by Woodhouse (1981). The details of this procedure are discussed in Text S2 of the supplemental material.

Earth model

In order to compute Δ and T using eqs. (1) and (2), the density ρ and five independent elastic constants for solid TI media (A, C, F, L, N) are required.

The constitutive relation for a TI medium is as follows:

$$\begin{pmatrix} \sigma_{xx} \\ \sigma_{yy} \\ \sigma_{zz} \\ \sigma_{xz} \\ \sigma_{yz} \\ \sigma_{xy} \end{pmatrix} = \begin{pmatrix} A & H & F & & & \\ H & A & F & & & \\ F & F & C & & & \\ & & & L & & \\ & & & & L & \\ & & & & & N \end{pmatrix} \begin{pmatrix} e_{xx} \\ e_{yy} \\ e_{zz} \\ 2e_{xz} \\ 2e_{yz} \\ 2e_{xy} \end{pmatrix}, \tag{5}$$

where

$$H = A - 2N. \tag{6}$$

The five independent elastic constants, A, C, F, L, and N, must be chosen so that the strain energy density is positive definite. This can be verified for any particular set of elastic constants by computing the principal minors of the strain energy tensor (the matrix in eq. 5). For an isotropic medium the relations between the above five elastic constants and λ and μ are as follows:

$$\lambda + 2\mu = A = C \tag{7}$$

$$\mu = L = N \tag{8}$$

$$\lambda = F = H. \tag{9}$$

The "PolynomialStructure" form (see Text S3 of the supplemental material) is one of two permissible formats to specify the input parameters to *ANISOtime*, ρ, V_{PV}, V_{PH}, V_{SV}, V_{SH}, and η, as cubic functions of radius. This allows an analytical computation of the turning point of a raypath by solving a cubic equation. The "PolynomialStructure" form also specifies the shear, and bulk attenuation coefficients Q_μ, and Q_κ, respectively. The attenuation coefficients are not used by *ANISOtime*, but should be included in the input parameter file so that users can use the same input file for *ANISOtime* and for the Direct Solution Method waveform computation software (DSM; Kawai et al., 2006). The standard definitions of V_{PV}, etc., are used (e.g., Panning and Romanowicz, 2006):

$$
\begin{aligned}
V_{PH} &= \sqrt{A/\rho} && (10)\\
V_{PV} &= \sqrt{C/\rho} && (11)\\
V_{SH} &= \sqrt{N/\rho} && (12)\\
V_{SV} &= \sqrt{L/\rho} && (13)\\
\eta &= \frac{F}{A-2L} && (14)
\end{aligned}
$$

In *ANISOtime*, the anisotropic and isotropic Preliminary Reference Earth Models (PREM: Dziewonski and Anderson, 1981) and AK135 model (Kennett *et al.*, 1995) are embedded in the program in "PolynomialStructure" form. When using *ANISOtime* in CLI mode, these models can be called using the argument values "prem," "iprem," and "ak135." We also support an input model format called "Named Discontinuity" (see Text S4 of the supplemental material) in the *TauP* toolkit (Crotwell *et al.*, 1999). At present, all models must have an Earth-like structure with a "mantle" (i.e., a solid outer region), underlain by an "outer core" (i.e., a liquid region), with an "inner core" (i.e., another solid region) at the center. Each of these regions can be arbitrarily vertically heterogeneous; i.e., the solid outer region ("mantle") can actually consist of a crust underlain by an upper mantle, transition zone, etc. The "outer core" must have zero shear modulus ($V_{SH} = V_{SV} = 0$), while the other regions must have strictly positive velocities and density. Models must specify the radius of the core-mantle boundary (CMB) and the inner-core boundary (ICB). Any model that satisfies the above conditions can be used.

Phases and distance

The rules for possible phase names follow those of the *Taup Toolkit* (Crotwell *et al.*, 1999). Symbols that describe wave types and interactions are listed in Table 2.

For most of the phases, the naming follows conventions used in global seismology. One distinction is that phase names must specify all the individual branches of the raypath (together with interactions at internal boundaries). For instance, the ScS2 phase, which bounces two times at the core-mantle boundary (tracing a 'W' in the mantle), is named 'ScSScS.' Another distinction is for phases that reflect at internal discontinuities other than the core-mantle boundary or the inner-core, which must be specified using a 'v' for a topside reflection, or a hat '^' for an underside reflection, followed by the depth of the internal discontinuity. For instance, an S phase with a topside reflection at the 670 km discontinuity in PREM is named 'Sv670S.'

For phases for which all branches are S phases (e.g., S, ScS, ScSScS, SS), *ANISOtime* allows the user to specify the polarization (SH or SV). The polarization is not specified in the phase name, but rather by using the options '-SV' and '-SH' in the command line (see section "CLI," below), or by switching the polarization in the GUI. The S branches for phases that include a P branch (e.g., SKS, ScP) will always have only SV polarization, and an error will result if the user tries to use the '-SH' option with such phases.

The epicentral distance computed by *ANISOtime* is the distance along the Earth's surface for the whole raypath. Although raypaths can have an epicentral distance of 360° or larger, *ANISOtime* does not make computations for such phases at present.

ABOUT *ANISOtime*

ANISOtime has both command line interface (CLI) and graphical user interface (GUI) modes. Both are similar to those used by the *TauP Toolkit*. There are some features which *TauP* can handle but *ANISOtime* cannot yet. We have no plans for any further development of the program, but will try to respond if there is a strong demand from users. *ANISOtime* automatically downloads and installs updates when there is a new release.

INSTALLATION

Java 8, or a more recent version, must be installed in order to run *ANISOtime*. Users can verify their Java environment by accessing https://www.java.com/en/download/installed8.jsp.

ANISOtime can be downloaded from https://github.com/UT-GlobalSeismology/anisotime. Downloadable executable versions are available for Windows, macOS, and Unix/Linux; the source code can also be downloaded. A user guide can be downloaded from this site, and is also embedded in the software.

CLI

When launched with arguments, *ANISOtime* runs in CLI mode. For instance, to compute and output an image of an SH phase raypath from a seismic source at a depth of 500 km at an epicentral distance of 60° propagating in the (anisotropic) PREM model, the arguments are "-h 500 -deg 60 -ph S -mod prem -eps -o

/path/to," which are identical to the arguments in TauP (except for the -eps and -o options). This will return the traveltime and create an eps file of the raypath in folder "/path/to."

```
% anisotime -h 500 -deg 60 -ph S -mod prem -eps -o /path/to
```

To obtain the traveltime and raypath for a pseudo-SV phase, the additional argument "-SV" should be used.

```
% anisotime -h 500 -deg 60 -ph S -mod prem -SV -eps -o /path/to
```

The full list of arguments can be obtained from the command "anisotime -help," and is given in Table 3.

RECORD SECTION

To draw a traveltime curve or create a record section, there must be sets of traveltime and epicentral distance values. Here is an example for the computation for pseudo-P-, pseudo-SV-, and SH-waves in PREM for the epicentral distance range $30° \leq \Delta \leq 60°$ with interval 5° for a source depth of 0 km:

```
% anisotime -rs 30,60,5 -h 0 -ph P,S -mod prem -o /path/to
```

Other examples can be found in the user guide.

GUI

When *ANISOtime* is launched without any arguments, it launches in GUI mode.

```
% anisotime
```

The GUI has 2 computational modes:

1. Epicentral distance mode
2. Ray parameter mode.

In either mode, the user must select seismic phases, epicentral distance, structure model and the depth of the source. Note that other parameters can also be changed. In epicentral distance mode, the epicentral distance is specified and raypaths are computed for that value, while in ray parameter mode raypaths are computed for the specified input ray parameter. Figs. 1 and 2 show results for epicentral distance mode and ray parameter mode, respectively.

END USER LICENSE AGREEMENT (EULA)

The software is licensed under the GNU General Public License (GPL), Version 3.0 (https://www.gnu.org/licenses/gpl-3.0.en.html.) After downloading *ANISOtime*, users must accept an End User License Agreement (EULA) before it can be launched. The main points of the EULA are that users agree to comply with the GPL in the event they use parts or all of our software in other works, and that they waive all possible claims in the event of problems with the software. This brief description is purely informal; the sole and binding agreement is that in the EULA itself. The authors welcome questions and bug reports to ut-globalseis@googlegroups.com and will respond if possible, but make no legally binding promise to do so.

RAYPATH CATALOG

When the ray parameter p is chosen, the raypath (for a given Earth structure) is determined, and so are both the epicentral distance Δ and the traveltime T for the raypath. Although the traveltime T and epicentral distance Δ can be directly computed for a particular ray parameter, most users want the traveltime T for a particular epicentral distance Δ. Since we cannot obtain the traveltime T or ray parameter p directly from the epicentral distance Δ, we must first find a ray parameter for a target epicentral distance Δ and then compute the traveltime T for the ray parameter p. In many cases, users require many pairs of T and Δ. In order to reduce the computational time, *ANISOtime* first computes sets of ray parameters p and corresponding epicentral distances Δ (i.e., a catalog) for a given structure, so that it can look for the ray parameter p which gives an epicentral distance Δ chosen by the user. When a user computes traveltimes for a new structure, the catalog for the structure will automatically be stored and used for later calculations.

VALIDITY CHECKS

Comparison to *TauP*

To verify the accuracy of the *ANISOtime* package, we first compare it to *TauP* for the case of isotropic PREM. Fig. 3 shows the difference of computed traveltimes for the default phases (S, P, ScS, PcP, SKS, PKP, SKiKS, and PKiKP) for a source at the Earth's surface. Fig. 3a shows the traveltime differences when using the default PREM of *TauP* (for which the depth grid intervals are between 15–100 km). Excluding the region around 25°, which corresponds to S and P phase triplications, thetraveltime difference for all phases is within 0.06 s. This relatively large discrepancy is due to the fact that the default accuracy of *ANISOtime* is better than that for *TauP*. Traveltime comparisons using a higher accuracy calculation for *TauP* are shown in Fig. 3b. The higher accuracy calculation is obtained by using an input layered velocity structure with finer depth sampling (6.371 km) than that for the default isotropic PREM in *TauP*. The traveltime differences for the higher-accuracy *TauP* calculations are within 0.0116 s of *ANISOtime* for all default phases for the entire epicentral distance range, and within 0.0016 s when excluding the regions near S wave triplications (around 25°). This is more than one order of magnitude smaller than the errors for the default PREM of *TauP*. In summary, *ANISOtime* and *TauP* are in good agreement for highly accurate calculations.

Comparison to an analytical solution

An analytical solution can be found for the TI medium with the elastic constants and density defined below:

$$A(r) = A_0 r^2 \tag{15}$$

$$C(r) = C_0 r^2 \tag{16}$$

$$L(r) = L_0 r^2 \tag{17}$$

$$N(r) = N_0 r^2 \tag{18}$$

$$F(r) = F_0 r^2 \tag{19}$$

$$\rho = \text{constant.} \tag{20}$$

We present a derivation in Text S5 of the supplemental material. As far as we know, this result is new for the spherically symmetric case, but it follows straightforwardly from well known results for the Cartesian case (Shearer and Chapman, 1988; Červený, 1989). We use this analytical solution to check the accuracy of the numerical traveltime integrals. Note that the medium defined in eqs. (15)-(20) has velocities that decrease linearly with depth. This is not a physically realistic model, but it is the only one for which an analytic solution is available for checking the numerical computations.

For the above medium, the traveltime between radius r_1 and r_2 is given by

$$T(p) = \int_{r_1}^{r_2} q_T(r,p)\ dr = q_{T0} \ln \frac{r_2}{r_1}, \tag{21}$$

where q_{T0} depends on the polarization (SH, pseudo-SV, or pseudo-P) and is given in Text S5 of the supplemental material.

We compute the difference between the traveltime for the ScS (SH), ScS (pseudo-SV), and pseudo-PcP phases computed using *ANISOtime*, and that computed using the analytical solution eq. (21) for the medium whose properties are defined in eqs. (15)-(20) with $A_0 = 7.55 \cdot 10^{-5}$, $C_0 = 7.12 \cdot 10^{-5}$, $F_0 = 2.63 \cdot 10^{-5}$, $L_0 = 2.46 \cdot 10^{-5}$, $N_0 = 2.61 \cdot 10^{-5}$, where A_0, C_0, F_0, L_0, and N_0 are in $\mathrm{Pa/m^2} = \mathrm{kg\ m^{-3}\ s^{-2}}$, and $\rho = 10\ \mathrm{kg/m^3}$. Note that the units of $A_0 \ldots$ are $\mathrm{Pa/m^2}$ rather than Pa, because, as shown by eqs. (15)-(19), the elastic constants are obtained by multiplying by r^2, which has units of m^2. The relative errors (defined below in eq. 22) using a constant integration mesh with 1 km spacing are $2.4490 \cdot 10^{-11}$, $2.4489 \cdot 10^{-11}$, and $2.4492 \cdot 10^{-11}$, for the ScS (SH), ScS (pseudo-SV), and pseudo-PcP phases, respectively.

$$\text{relative error} = \frac{T_{ANISOtime} - T_{analytical}}{T_{analytical}} \tag{22}$$

Comparison to full-wave theory

To further test the accuracy of *ANISOtime*, we compare the traveltime predicted by *ANISOtime* to the arrival time on waveforms computed using full-wave theory for realistic isotropic and transversely isotropic media. The synthetic waveforms are computed using the Direct Solution Method (Kawai *et al.*, 2006) up to 2 Hz for an event at depth 571.3 km. The Earth models used are PREM, isotropic PREM, and MIASP91ANI, a modified version of IASP91 with smoothed upper mantle discontinuities and 1% V_{SV} and 3% V_{SH} increases, respectively, in the lowermost 250 km of the mantle (see Fig. 4). In order to avoid the effects of velocity dispersion, we set $Q_\mu = 5000$, and $Q_\kappa = 57823$, i.e., essentially an elastic medium, to compute the synthetics using the DSM (which requires non-zero values for the anelastic parameters). Velocity dispersion reduces the velocity for frequencies lower than a reference frequency (typically 1 Hz), and would delay the arrival of seismic pulses on the synthetics, thereby inducing disagreement with *ANISOtime*. The waveforms are low-pass filtered with a corner frequency of 0.25 Hz.

The synthetics and traveltime curves are shown in Figs. 5, 6, 7 and 8. Fig. 5 shows a record section and traveltime curves for the SH (transverse component) and pseudo-SV (radial component) phases that sample the D$''$ layer for the model in Fig. 4c. The onset times of the SH and pseudo-SV phases, and the triplicated arrivals due to the D$''$ discontinuity, are well reproduced by *ANISOtime*. Figs. 6, and 7 show a larger set of phases on three-component synthetics for isotropic PREM (Fig. 4a), and closeups of some specific phases for clarity, respectively. Fig. 8 shows record sections for the S and pseudo-P phases that sample the upper mantle and mantle transition zone for the (anisotropic) PREM model (Fig. 4b).

We quantify the agreement between the full-wave synthetics and *ANISOtime* in Fig. 9. Fig. 9 shows the difference between traveltimes predicted using *ANISOtime*, and manually-picked onset times for the direct SH and pseudo-P phases and waveforms for the isotropic (Fig. 6) and anisotropic (Fig. 8) PREM models. Traveltime discrepancies are within 0.2 s (except for 5 points for the SH phase at small epicentral distances, where the onset time is not clear because of triplicated phases), with average differences for the SH phase of -0.06 s, and -0.03 s, and -0.07 s, and -0.07 s for the pseudo-P phase, for the isotropic and anisotropic PREM models, respectively. We note that we only picked the SH and pseudo-P phases, since these are direct phases. Other later phases (or the direct SV phase) have precursors before the onset of the main phases (due to internal, e.g., crustal, reflections, or S-to-P conversions); this makes it difficult to pick precise onset times. However, we expect later pseudo-P as well as pseudo-SV phases to have similar levels of agreement, since later phases are combinations of S and P branches, and the equation for the traveltime of the pseudo-SV phase is the same as that for the pseudo-P phase, except for a difference in sign in one term (see eq. S69 in the supplemental material). For these later phases, the agreement with *ANISOtime* can be visually checked in Figs. 5, 7, and 8.

DATA AND RESOURCES

We used no data. Parameters for the three Earth models embedded in *ANISOtime* (PREM, isotropic PREM, and AK135) are available from IRIS Data Services http://ds.iris.edu/ds/products/emc-referencemodels/. The supplemental material consists of the following five Texts. Text S1: Theory for laterally homogeneous, transversely isotropic, media; Text S2: Integration near the turning point; Text S3: "PolynomialStructure" file; Text S4: "Named Discontinuity" file; Text S5: Analytical solution for a spherically symmetric, TI, medium with constant velocity gradient.

ACKNOWLEDGMENTS

This research was partly supported by grants from the Japan Society for the Promotion of Science (Nos. 16K05531, 15K17744, 15H05832, and 18K03797). We thank Jeroen Ritsema, the other referee, and the associate editor for their constructive comments on the original manuscript.

REFERENCES

Borgeaud, A. F. E., K. Konishi, K. Kawai, and R. J. Geller (2016). Finite frequency effects on apparent S-wave splitting in the D'' layer: comparison between ray theory and full-wave synthetics, *Geophys. J. Int.* **207**, 12–28, doi: 10.1093/gji/ggw254.

Červený, V. (1989). Ray tracing in factorized anisotropic inhomogeneous media, *Geophys. J. Int.* **99**, 91–100, doi: 10.1111/j.1365-246X.1989.tb02017.x.

Crampin, S. (1981). A review of wave motion in anisotropic and cracked elastic-media, *Wave Motion* **3**, 343–391. https://doi.org/10.1016/0165-2125(81)90026-3

Crotwell, H. P., T. J Owens, and J. Ritsema (1999). The TauP toolkit: flexible seismic travel-time and ray-path utilities, *Seismol. Res. Lett.* **70**, 154–160, doi: 10.1785/gssrl.70.2.154.

Dziewonski, A. M., and D. L. Anderson (1981). Preliminary reference Earth model, *Phys. Earth Planet. Inter.* **25**, 297–356, doi: 10.1016/0031-9201(81)90046-7.

Jeffreys, H., and B. S. Jeffreys (1956). *Methods of Mathematical Physics*, 3rd ed., Cambridge University Press, doi:10.1017/CBO9781139168489.

Kawai, K., N. Takeuchi, and R.J. Geller (2006). Complete synthetic seismograms up to 2 hz for transversely isotropic spherically symmetric media, *Geophys. J. Int.* **164**, 411–424, doi: 10.1111/j.1365-246X.2005.02829.x.

Kennett, B. L. N., and E. R. Engdahl (1991). Travel times for global earthquake location and phase identification, *Geophys. J. Int.* **105**, 429–465, doi: doi.org/10.1111/j.1365-246X.1991.tb06724.x.

Kennett, B. L. N., E. R. Engdahl, and R. Buland (1995). Constraints on seismic velocities in the Earth from traveltimes, *Geophys. J. Int.* **122**, 108–124, doi: 10.1111/j.1365-246X.1995.tb03540.x.

Love, A. E. H. (1927). A Treatise on the Mathematical Theory of Elasticity 4th ed., *Cambridge University Press.*

Panning, M., and B. Romanowicz (2006). A three-dimensional radially anisotropic model of shear velocity in the whole mantle, *Geophys. J. Int.* **167**, 361–379, doi: 10.1111/j.1365-246X.2006.03100.x.

Shearer P. M., and C. H. Chapman (1988). Ray tracing in anisotropic media with a linear gradient, *Geophys. J.* **94**, 575–580, doi: 10.1111/j.1365-246X.1988.tb02277.x.

Vlaar, N. J. (1968). Ray theory for an anisotropic inhomogeneous elastic medium, *Bull. Seism. Soc. Am.* **58**, 2053–2072.

Vlaar, N. J. (1969). Rays and travel times in a spherical anisotropic earth, *Bull. Seism. Soc. Am.* **59**, 1051–1060.

Woodhouse, J. H. (1981). A note on the calculation of travel times in a transversely isotropic Earth model, *Phys. Earth Planet. Inter.* **25**, 357–359, doi: 10.1016/0031-9201(81)90047-9.

K. Konishi, and A.F.E. Borgeaud
Institute of Earth Sciences
Academia Sinica
128 Academia Road, Section 2, Nangang, Taipei 11529
Taiwan

A.F.E. Borgeaud, K. Kawai, and R.J. Geller
Department of Earth and Planetary Science
School of Science
University of Tokyo
Hongo 7-3-1, Bunkyo-ku, Tokyo 113-0033
Japan

Table 1: Variables used in main body of paper (in order of appearance).

Variable	Meaning	Units	Where defined
T	traveltime	s	before eq. (1)
Δ	epicentral distance	radian	before eq. (1)
p	ray parameter for spherical Earth	s/radian	eq. (S70)
r	radius in spherical polar coordinates	km	before eq. (1)
$q_\Delta(p,r)$	kernel for epicentral distance	radian/km	eqs. (S75)–(S77)
$q_T(p,r)$	kernel for traveltime	s/km	eqs. (S72)–(S74)
A, C, F, L, N	elastic constants for VTI medium	N/m^2	eqs. (5)–(9)
V_{PH}, V_{PV}, V_{SH}, V_{SV}	velocity-like quantities used as input to *ANISOtime*	km/s	eqs. (10)–(13)
η	quantity used as input to *ANISOtime* to fully specify the five elastic constants	dimensionless	eq. (14)

Note: Variables used only in the supplemental material are not included in the above table

Table 2: Description of symbols for seismic phases.

Symbols	Wave type
P	P-wave, upgoing or downgoing, in the mantle
p	upgoing P-wave from a seismic source
S	S-wave, upgoing or downgoing, in the mantle
s	upgoing S-wave from a seismic source
K	P-wave in the outer core
I	P-wave in the inner core
J	S-wave in the inner core
	Interactions
c	topside reflection off the core-mantle boundary
i	topside reflection off the inner-core/outer-core boundary
ˆ	underside reflection, used primarily for crustal and mantle interfaces
v	topside reflection, used primarily for crustal and mantle interfaces
diff	appended to P or S to represent a diffracted wave along the core-mantle boundary

Author's note to copy editor:

Because the upper half and lower half of the table show different things, please do not delete any of the horizontal lines in this table, even though this differs slightly from the usual conventions for typesetting tables.

Table 3: List of arguments for *ANISOtime* CLI.

Parameter	Meaning
-dec	Number of decimal places for output
-deg	Epicentral distance Δ [deg]
-h	Depth of source [km] (default:0)
-mod	Structure: prem, iprem, ak135, or path to "PolynomialStructure" or "Named Discontinuity" file (default:prem).
-help	Prints the usage. This option has the highest priority
-ph, --phase	Seismic phases (default:P,PCP,PKiKP,S,ScS,SKiKS)
-p	Ray parameter [s/deg]
--version	Shows version information. This option has the 2nd highest priority
-SH	Computes traveltime for SH (default:SH)
-SV	Computes traveltime for SV (default:SH)
-dD	Parameter for catalog creation (dΔ)
-dR	Integral interval [km] (default:10.0)
-eps	Output path figure
-o	Output file for a record section. If it already exists, an error will be raised
--delta	Show only epicentral distances
--rayp	Show only ray parameters
--time	Show only traveltimes
--taup	Use the same output format as *taup_time*
-rc, --read-catalog	Path of a catalog for which traveltimes are computed
-rs, --record-section	start,end(,interval) [deg] Computes a table of a record section for the range

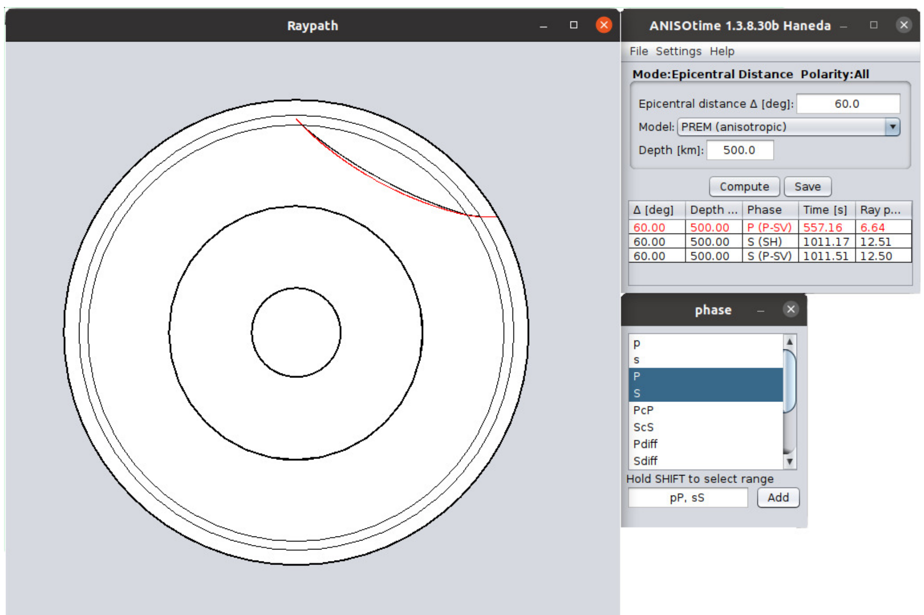

Figure 1: Sample figure made in epicentral distance mode. P- and S-waves with an epicentral distance of 60° are computed. The figure has been edited to remove the gray background in the raypath window.

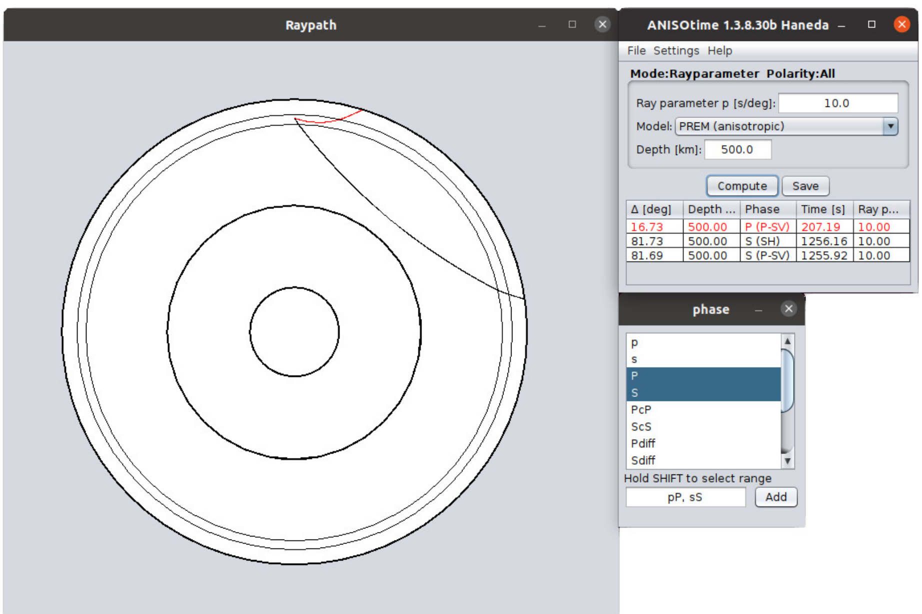

Figure 2: Sample figure made in ray parameter mode. P- and S-waves with a ray parameter of $p = 10$ s/degree are computed. The figure has been edited to remove the gray background in the raypath window.

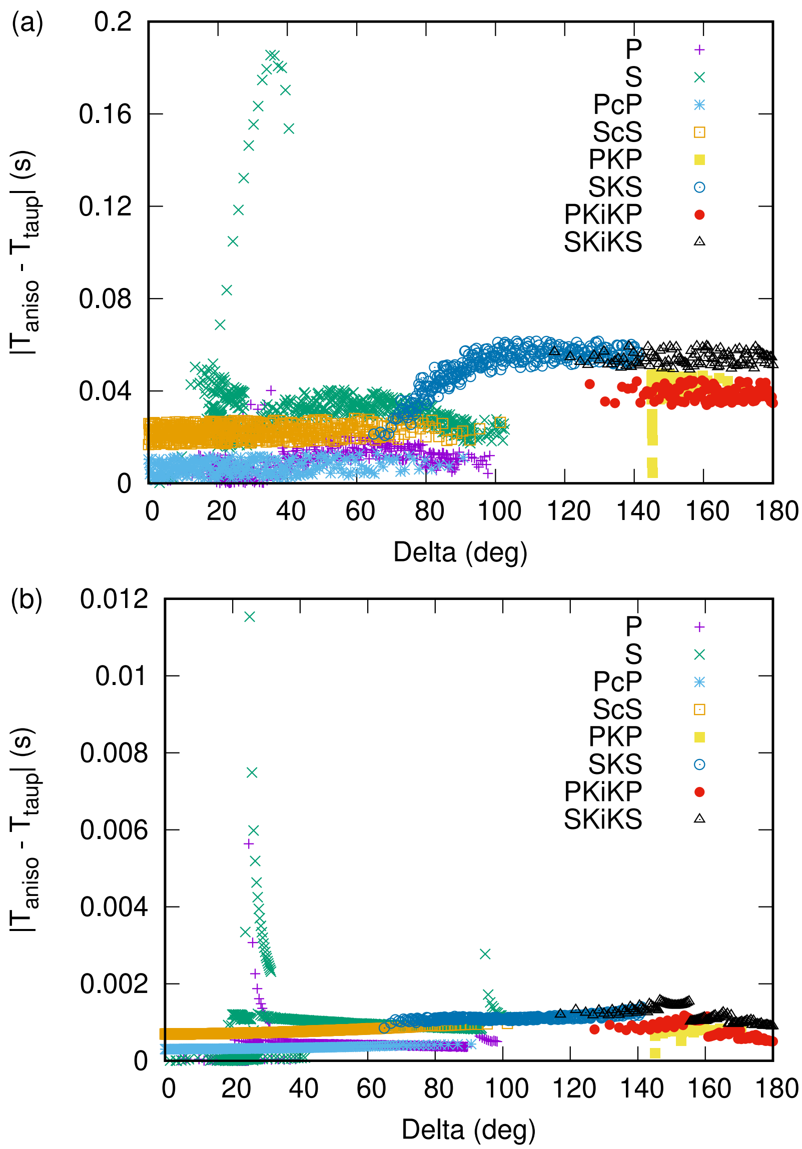

Figure 3: Absolute difference between traveltimes computed using *ANISOtime* and *TauP* for all default phases for a source at the Earth's surface. The model used to compute traveltimes with *ANISOtime* is isotropic PREM "PolynomialStructure." The model used to compute traveltimes with TauP are a) the default (isotropic) PREM included in the *TauP* package; b) isotropic PREM, but with a finer depth sampling, resulting in increased accuracy as compared to traveltimes computed with the *TauP* default model (see text for details).

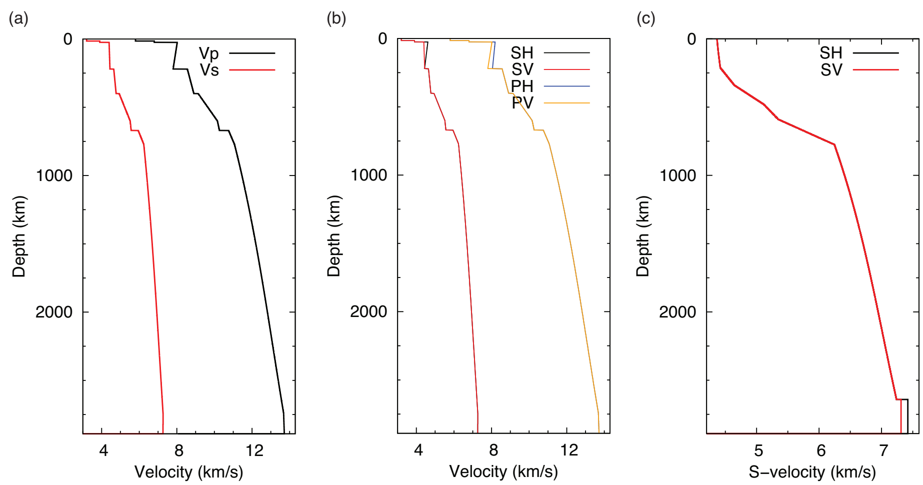

Figure 4: Models used to test *ANISOtime*. (a): isotropic PREM; (b) anisotropic PREM, with SH and PH velocities faster than SV and PV velocities, respectively, between 24 and 220 km depth; (c) MIASP91ANI, a modified version of IASP91 (Kennett and Engdahl, 1991) with smoothed discontinuities in the upper mantle (Borgeaud *et al.*, 2016) with SH velocity increased by 3%, and SV velocity increased by 1% in the lowermost 250 km of the mantle.

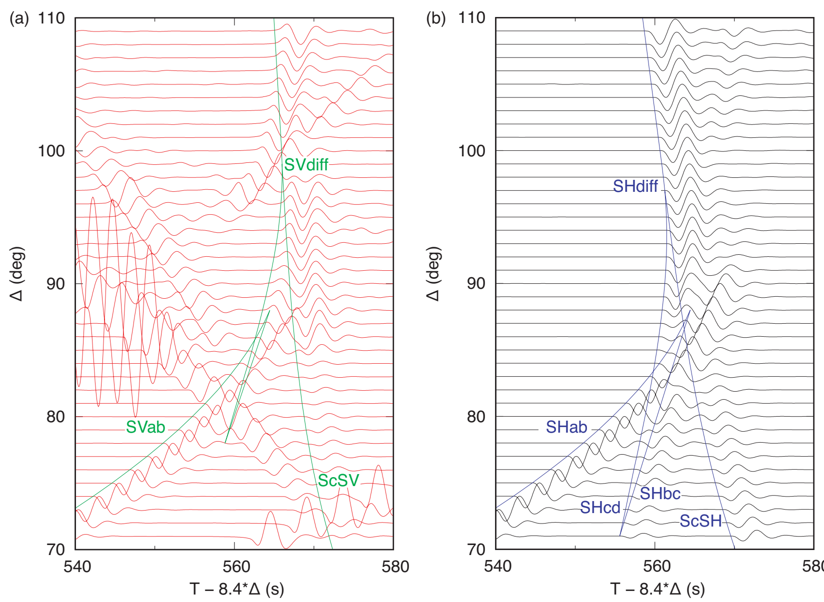

Figure 5: Waveforms for the radial (a) and transverse (b) components computed using the DSM for the anisotropic model in Fig. 4(c) for a source at 571.3 km depth. The traces are normalized using a time window around the S phase. The horizontal axis shows the reduced traveltime for a slowness of 8.4 s/degree. The traveltime curves for SV and SH waves (see labels), which were computed using *ANISOtime*, are in good general agreement with the synthetics.

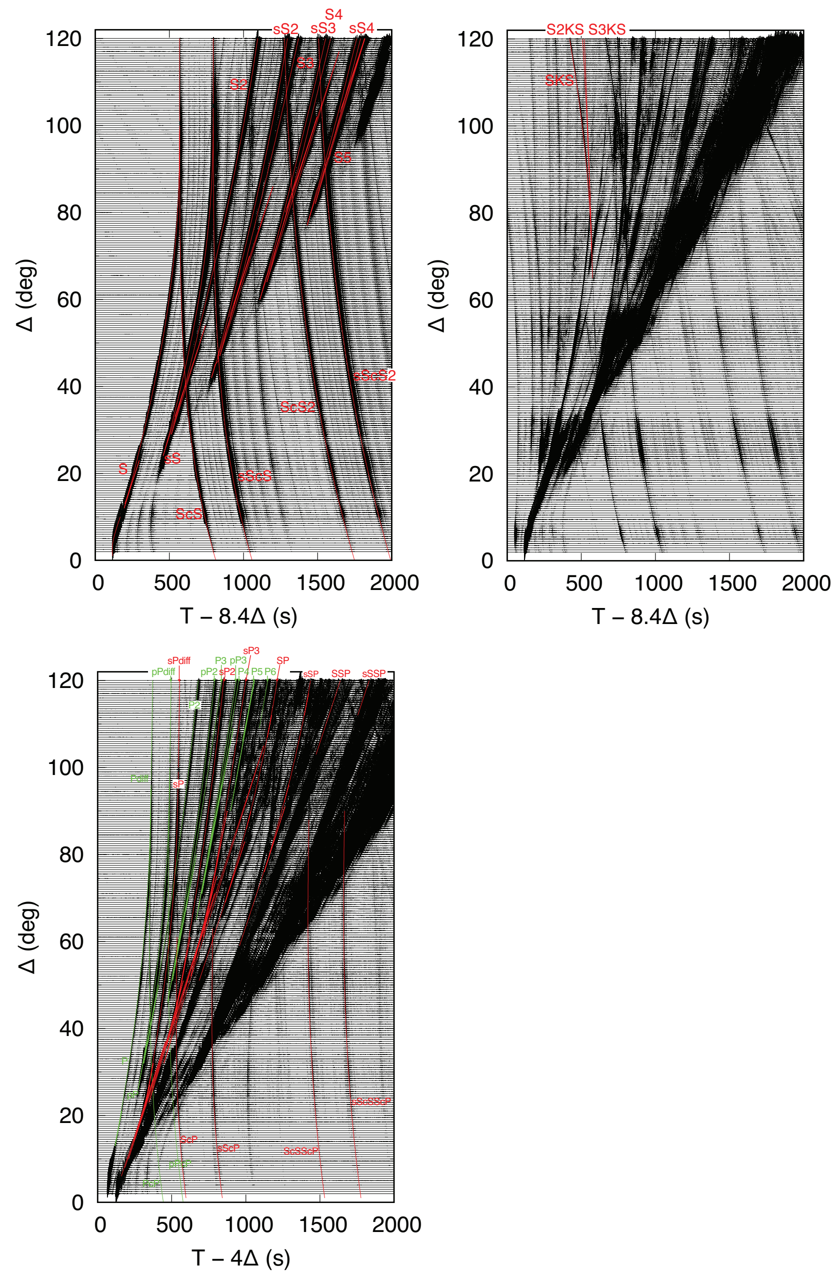

Figure 6: Waveforms for the transverse (a), radial (b), and vertical (c) components computed using the DSM for isotropic PREM (Fig. 4a) for a source at 571.3 km depth. The traces are self-normalized at each epicentral distance.

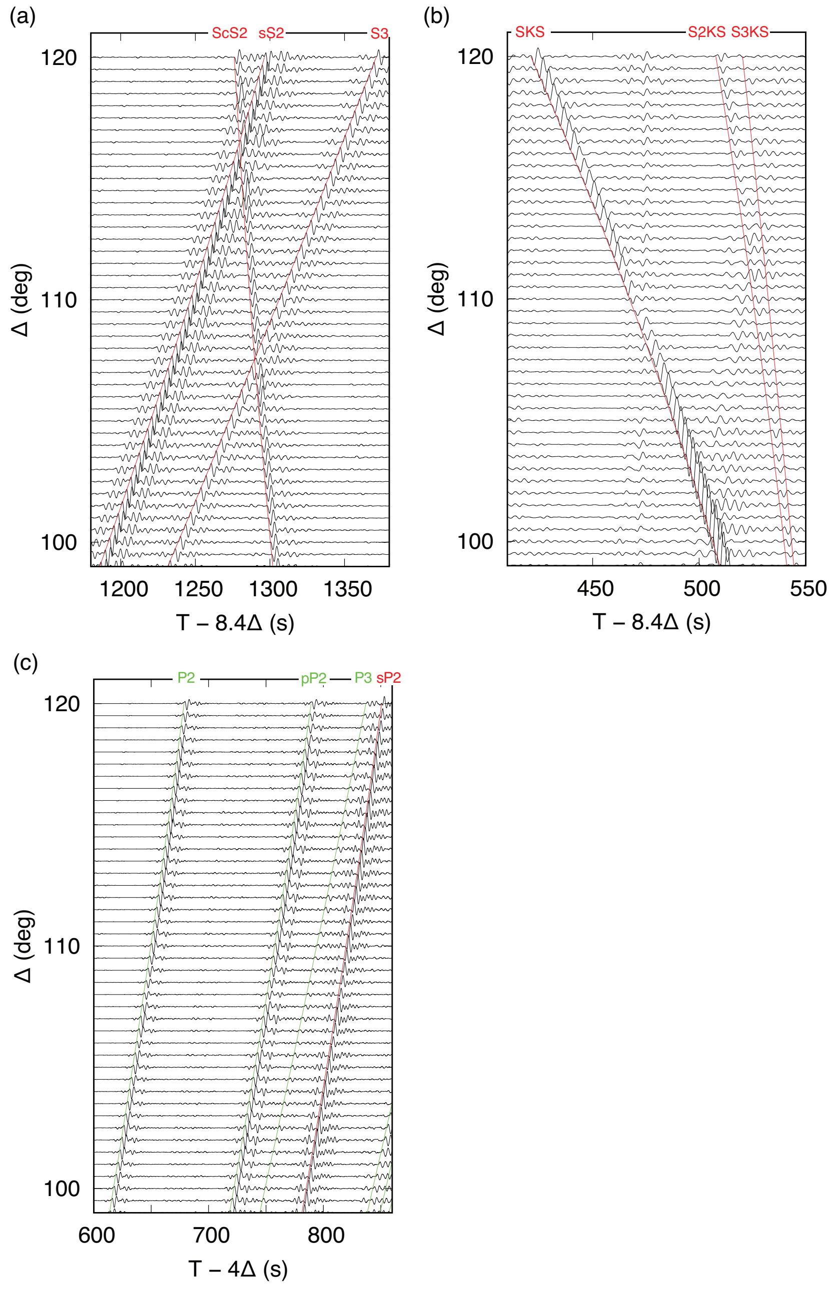

Figure 7: Closeups of the record sections in Fig. 6 showing epicentral distance range from 100 to 120 degrees, for the transverse (a), radial (b), and vertical (c) components.

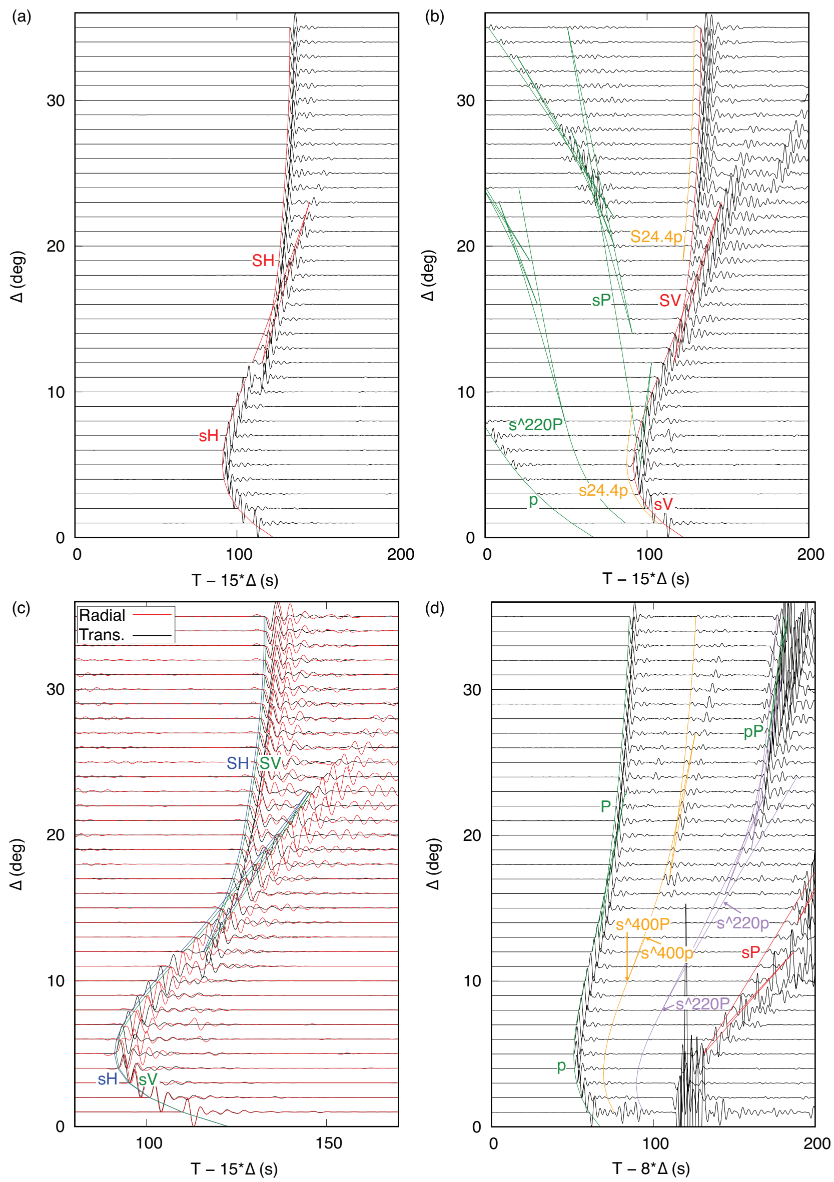

Figure 8: Waveforms computed using the DSM for anisotropic PREM (Fig. 4b) for a source at 571.3 km depth: a) transverse component; b) radial component; c) comparison of transverse and radial components; d) vertical component. The traces are normalized using time windows around the S phase (panels a, b, and c), and around the pseudo-P phase (panel d).

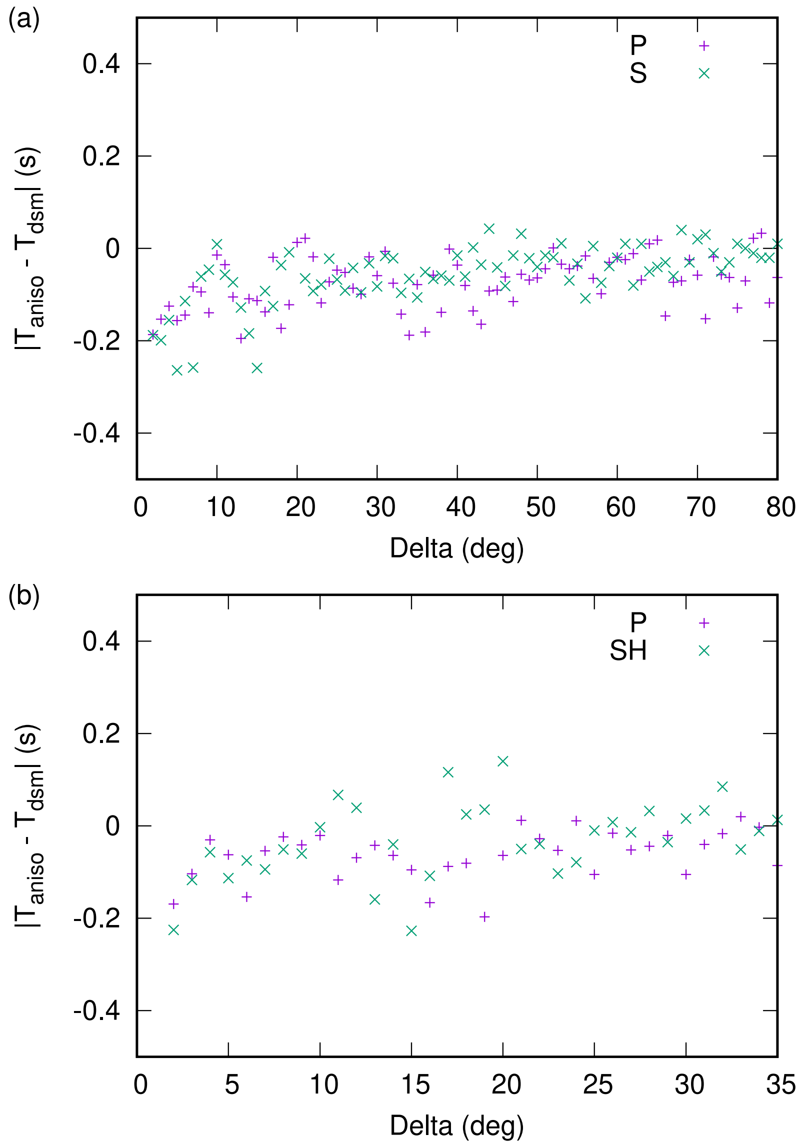

Figure 9: Differences between traveltimes computed using *ANISOtime* and onset times picked on synthetic waveforms for a) the isotropic PREM model (Fig. 6), and b) the anisotropic PREM model (Fig. 8) for the pseudo-P and SH phases.